Simulation of a Standard Store Separated from Generic Wing

M. Sheharyar [1†], E. Uddin [1], Z. Ali[1], Q. Zaheer[2] and A. Mubashar[3]

[1] *Department of Mechanical Engineering, SMME, NUST, Islamabad 44000, Pakistan*
[2] *College of Aeronautical Engineering, NUST, Islamabad 44000, Pakistan*
[3] *Mechanical Engineering Program, Middle East Technical University Northern Cyprus Campus, Mersin, Turkey*

†*Corresponding Author Email: muhammadsheharyar86@gmail.com*

ABSTRACT

Evaluation of store separation experimentally is expensive; time consuming and dangerous as human risks are involved. This results in development of computational methods to simulate the store separation. Store separation studies include store separation simulation and determination of linear and angular displacements of store under the influence of complex and non-uniform flow field of parent aircraft. In order to validate the methodology, the unsteady CFD results, obtained by coupling six degrees of freedom (6-DOF) with flow solver, are compared with experimental results. Major trends are captured which are consistent with experimental results. Variation in store trajectory has been evaluated with different combinations of forward and rearward ejection forces. By increasing the magnitude of forward ejection force vertical displacement increases and store separates more safely from the wing. Moreover, effects of varying parent wing configuration on store trajectory has also been analyzed by incorporation of leading-edge flaps (LEFs). Store always separates in nose down condition due to LEFs which increases vertical displacement of store and thus safety related to store separation is enhanced.

NOMENCLATURE

CFD	computational fluid dynamics	Phi	roll angle of the store in deg
G	gravity	Psi	yaw angle of the store in deg
I_{xx}	roll moment of inertia	Theta	pitch angle of the store in deg
I_{yy}	pitch moment of inertia	X	X is positive in direction of flight path
I_{zz}	yaw moment of inertia	X_{CG}	center of mass
L	store model length	Y	Y is positive to pilot's right
M	Mach number	Z	Z is positive downward

1. INTRODUCTION

Store separation tests have paramount importance in the certification of a new store on an aircraft. The main purpose of this test is to demonstrate the safe and effective deployment of the store. These tests don't only ensure the safe separation of a store but also it is a validation of airframe/store compatibility as shown by Covert (1981). Whenever a new store is introduced or an old one needs some modification it needs an airworthiness certification in order to be deployed on an aircraft. There are three main

approaches that have been used for store separation testing e.g. Wind tunnel testing, Flight testing and CFD analysis. Before wind tunnel testing and CFD analysis, flight testing was the only way to ensure that the said store is safe for deployment which was not only dangerous for the pilot flying the particular aircraft but also it could lead to the serious aircraft damage and this concept is well documented by Cenko (2010).
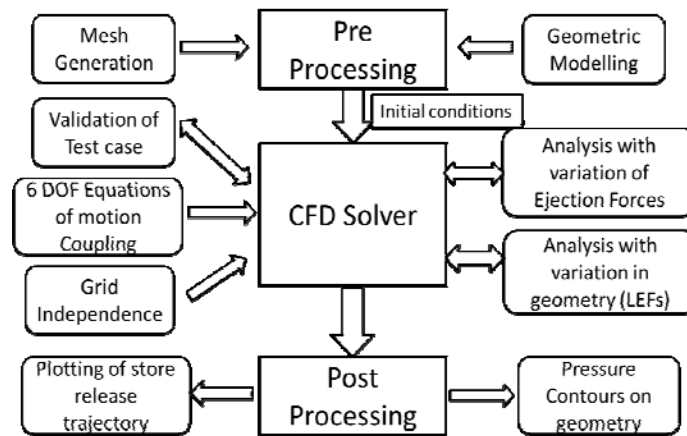
The importance of safe store separation has

Fig. 1. Numerical Methodology.

increased after the development of closed cockpit aircraft. A desire for having multiple stores on same wing has further amplified the significance of safe clearance. Whenever store separates from the aircraft during flight it is extremely required that it does not come in contact with aircraft or neighboring stores see Demir (2004). Store separation studies have been carried out to investigate the effect of flow field on the trajectory of store once it separates from the wing pylon. One of such study analyses the effect of fixed stores installed in the near vicinity of the under investigation separated store on the same wing. It was concluded shown by Demir and Alemdaroğlu (2015) that the neighboring fixed stores have no effect on the trajectory of separated store in lateral and longitudinal directions and it was.

The utility of computational methods for estimation of aerodynamic forces and the resultant trajectory of the separated store from a generic wing was analyzed using implicit Euler solver. The 6 DOF trajectory model was integrated with the solver. Several store separation cases were analyzed and the results were in good approximation with the experimental results. The parameters obtained using CFD code were then used as input to the autopilot model for commanded maneuvers of store. The feasibility of coupling the autopilot model with the CFD code was successfully demonstrated by Hall *et al.* (1997).

EGLIN test case was simulated using numerical solver, coupled with 6DOF trajectory model. After validation of CFD code with EGLIN test case, the trajectory of store was studied at supersonic Mach number (M=1.2). It was concluded by Sunay *et al.* (2013) that viscous effects have negligible influence on the trajectory of separated store. The effect of variation angle of attack and side slip angle on the body dynamics of weapon release from the generic wing was evaluated. It was observed that as the angle of attack increases the vertical drop rate of weapon decreases due to increase in vertical aerodynamic force. However, lateral motion of the released weapon was affected by the side slip angle see the work of Mahmood *et al.* (2018).

Safe release of external store from the wing pylon of an aircraft is of prime importance as far as the aerodynamic design parameters of store, magnitude of ejection forces and pylon geometrical design is concerned. Another aspect during the release of external store to be considered is the flow characteristics over the wing. The store separation phenomenon must not affect the aerodynamics of wing. From the literature survey, it is evident that the most significant contributor towards the trajectory estimation of separated store is the magnitude of ejection forces and moments as shown by Demir and Alemdaroğlu (2015). In this research study, the modelled store configuration is having two ejection points. The magnitude of ejection forces and moments is varied and their effect on store separation trajectory is analyzed. Furthermore, Leading Edge Flap has drastic effects on aerodynamic characteristics of wing as concluded by Sejong and Tavella (1987). In order to ascertain the effect of high lift devices on the store trajectory, wing geometric configuration is altered by introducing leading-edge flaps at different deflection angles.

2. NUMERICAL METHODOLOGY

Computational fluid dynamics software has been used for aerodynamic analysis of generic wing-pylon-store. The Navier-Stokes flow solver and six Degree of Freedom (DOF) equations are coupled. A density-based finite-volume solver for compressible flows is used. The solver incorporates higher-order numerical schemes (second order upwind discretization scheme) and advanced physical models to provide accurate and efficient solutions to complex engineering flow problems. This is augmented by a database which manages transport and thermodynamic properties of species and fluids as well as kinetic models for various applications. The predicted computed trajectories are compared with a 1/20 scale wind-tunnel experimental data conducted at the Arnold Engineering Development Center (AEDC) see work of E. R. Heim. (1991). The overall computational scheme of the analysis is shown in Fig. 1.
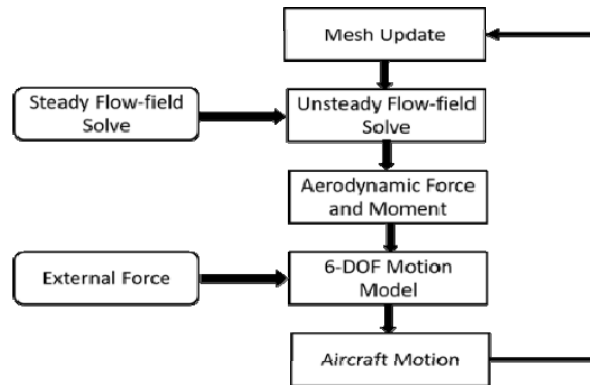
Fig. 2. Flowchart of coupling solve.

In order to validate the results i.e. center of gravity locations, center of gravity orientations, linear velocities and angular velocities obtained from the CFD analysis are compared with experimental results available in literature. After validation, the same geometry is tested at different combinations of front and rear ejection forces. Moreover, CFD analysis of store separation with leading-edge flaps installed on the wing at different deflection angles is also studied.

Governing equations for computational analysis are derived from the work of Bachelor (2000) and ANSYS Fluent® help. For steady state solution the conservation of mass is given by,

$$\frac{\partial p}{\partial t} + \nabla.\left(\rho \vec{v}\right) = S_m \qquad (1)$$

where ρ is the mixture density, $\vec{v}$ is the mass averaged velocity and S_m is source which is actually the mass added to the continuous phase form the dispersed second phase.

Similarly, equation for conservation of momentum in an inertial reference frame is given as: -

$$\frac{\partial}{\partial t}\left(\rho \vec{v}\right) + \nabla.\left(\rho \vec{v}\vec{v}\right) = -\nabla p + \nabla.\left(\overline{\overline{T}}\right) + \rho\vec{g} + \vec{F} \qquad (2)$$

where p is static pressure, $\overline{\overline{T}}$ is stress tensor, $\rho\vec{g}$ is gravitational body force, $\vec{F}$ is external body forces which arise from the interaction with the dispersed phase. By solving the above equation, we get the three different equations in the x, y and z directions which are called the Navier Stokes equations.

The Conservation of total energy per volume is,

$$\frac{\partial\left(\rho E\right)}{\partial t} + \nabla.\left(\vec{v}\left(\rho E + p\right)\right) = -\nabla.\left(\sum_j h_j J_j\right) + S_h \qquad (3)$$

Where E is the total energy per volume, h_j is the enthalpy, J_j is the diffusion flux of species and S_h includes the heat of chemical reaction.

The 6 DOF solver in ANSYS Fluent® uses the object's forces and moments in order to compute the translational and angular motion of the center of gravity of an object. The governing equation for the translational motion of the center of gravity is solved for in the inertial coordinate system.

$$\dot{\vec{v}}_G = \frac{1}{m}\sum \vec{f}_G \qquad (4)$$

where v_G is the translational motion of the center of gravity, m is the mass, and f_G is the force vector due to gravity.

The angular motion of the object, w_B is more easily computed using body coordinates:

$$\dot{\vec{\omega}}_B = L^{-1}\left(\sum \vec{M}_B - \vec{\omega}_B \times L\vec{\omega}_B\right) \qquad (5)$$

where L is the inertia tensor, M_B is the moment vector of the body, and w_B is the rigid body angular velocity vector.

The moments are transformed from inertial to body coordinates using

$$\vec{M}_B = R\vec{M}_G \qquad (6)$$

where, R represents the transformation matrix.

The translational equation, therefore, describes the aircraft with respect to its three translational degrees of freedom, while the rotational equation describes the aircraft with respect to its three rotational degrees of freedom. Newton's second law, therefore, yields six equations for the six degrees of freedom of a rigid body.

In order to predict store separation trajectory two set of equations i.e. Navier-Stokes equations and Equations of motion are to be solved simultaneously so there is a requirement of User Defined function (UDF) written in C language for coupling of above-mentioned set of equations. UDF is dynamically loaded with ANSYS Fluent® and used to define and pass the mass and inertial properties of the store and the ejector forces and moments to the six DOF solvers. The flow chart for the coupling solve is shown in Fig. 2:

3. COMPUTATIONAL SETUP

For the CFD analysis, a clipped delta wing having geometry of 45° leading edge sweep is used. Moreover, a standard store with four fins which are

arranged in a cruciform around the tail region with a constant airfoil shape NACA 0008 is attached to aircraft using a pylon as shown in Fig. 3. The model geometry is designed using the Pro-engineer design tool see the work of Fox (2000).
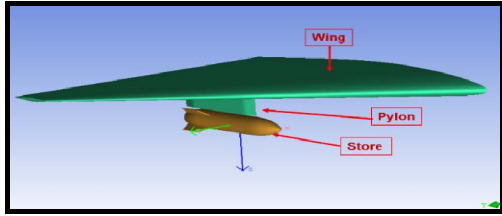

Fig. 3. Geometry of the wing/pylon/store.

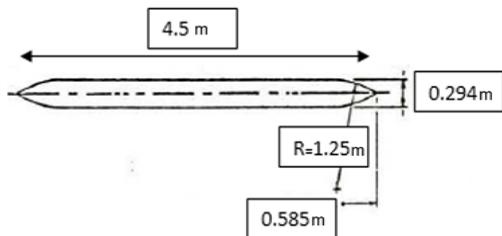Detailed geometry of wing, pylon and store is shown in Figs. 4 and 5: -

Fig. 4. Dimensions of the pylon.

ANSYS ICEM® is used to generate the unstructured computational grid for CFD analysis. In order to minimize the occurrence of negative volumes in the flow solver, an internal block was created around the store region. The boundary condition of the block is selected as interior. The initially generated grid contained 1657126 elements and 279835 nodes see the work of Parikh et al. (1992) as shown in Fig. 6.

Pressure Far Field is selected for downstream, upstream and all side boundaries but the inboard side boundary is selected as symmetry. The internal block is defined as interior whereas the solid surfaces are modeled as no slip, adiabatic wall boundary conditions. A test case of wing having store is used for the calculation of the trajectory of the store. The experiments which are used for the calculation of computational results were performed in the transonic (M=0.95) flow regime with an angle of attack of zero at 26000 ft. altitude from which the static pressure and temperature values were taken see the work of Koomullil et al. (2008).

Reynolds Averaged Navier Stokes (RANS) two equations standard k-ε model is used (Launder et al. 1974). The k-ε model was designed especially for aerospace applications involving wall-bounded flows and has been shown to give good results. Robustness, economy, and reasonable accuracy for a wide range of turbulent flows are some of the properties which contribute to its popularity for different simulations. Enhanced wall treatment options are also available with the k- ε model which is a near-wall modeling method that combines a two-layer model with enhanced wall functions and

is highly recommended with turbulent flows involving store separation.

The store/inertial mass properties and ejector parameters are given in Table 1.

Table 1 Store mass properties and Ejector parameters

Weight	907.185 Kg
Center of mass (X_{CG})	1.417 m
Roll moment of inertia(I_{xx})	27.116 kg.m^2
Pitch moment of inertia(I_{yy})	488.094 kg.m^2
Yaw moment of inertia(I_{zz})	488.094 kg.m^2
Forward ejector location	1.2375 m
Aft ejector location	1.7465 m
Forward ejector force	10.7 KN
Aft ejector force	42.7 KN

Mesh sensitivity studies has been carried out prior to detailed CFD analysis. The solution should be independent of number of cells in the grid. For this purpose, grid independence studies have been carried out. Three types of grids have been generated namely a course grid, a fine grid and an extra-fine grid. Drag comparisons for the three types of grids are given in Fig. 7. Grid independence is achieved at 1.6 million number of cells. So, this size of mesh is used for further CFD analysis.

4. RESULTS AND DISCUSSIONS

4.1 Solver Validation Test Case

Figure 8 shows the trajectory of center of gravity locations with respect to time as compared to the experimental data. When the store separates from the aircraft under the influence of gravity and ejector forces, the store begins to move backward, downward and inward. The inward and backward movements start after about t=0.17 seconds. It is apparent that vertical displacement matches very closely with the experimental data. This is because the ejector and gravity forces dominate the aerodynamic forces in this direction. The small discrepancy in the horizontal displacement is expected because the drag is underestimated due to viscous effects. Overall the linear displacements in all the three directions shows great agreement with the available experimental data.

Figure 9 shows the trajectory for center of gravity angular orientations with respect to time as compared to the experimental data. The store moves in a pitch up, yaw and right roll direction because of aerodynamic forces. The ejector forces act on the store till real time of t=0.052 seconds which is the main reason for the pitch up movement of the store. After being free from the influence of ejector forces then aerodynamic forces will define the motion of store that is why store starts to pitch down around t=0.19 seconds. The maximum pitch up angle calculated through CFD is 5.46 degrees whereas experimental data shows a maximum pitch up angle of 5.33 degrees.
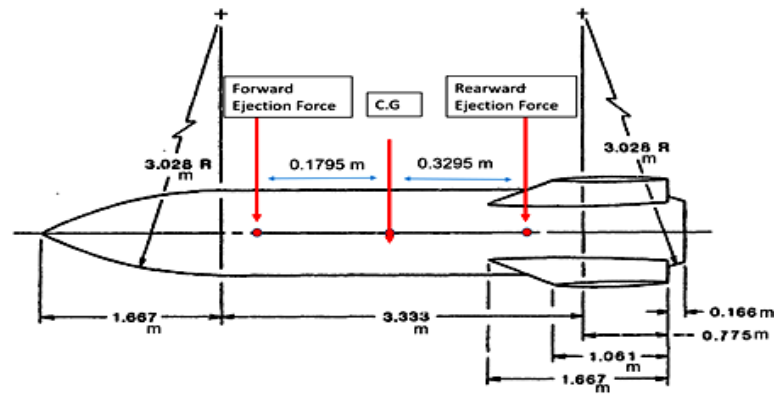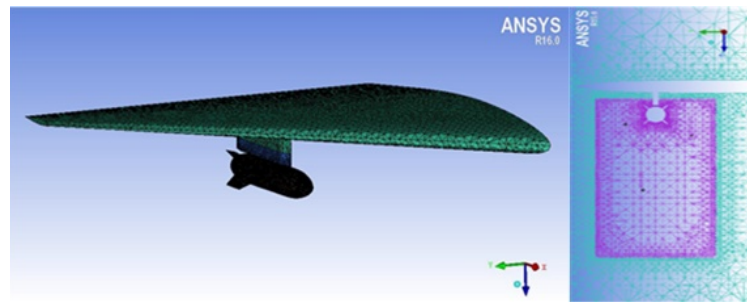
Fig. 5. Dimensions of the Store.

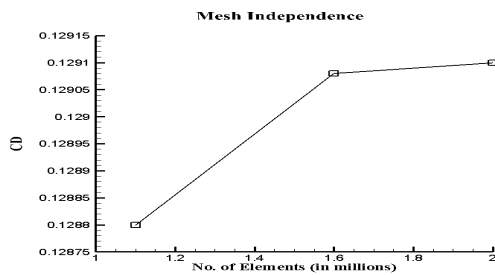**Fig. 6. Surface mesh (left) and mesh cut plane from front (right) of geometry.**

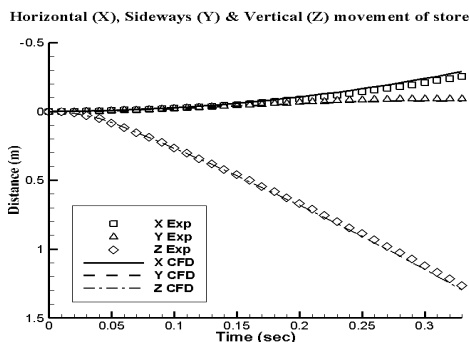**Fig. 7. Grid Independence graph.**

Fig. 8. Trajectory of the center of gravity locations (X, Y, Z).

The store rolls in the right-side direction after it is being separated from the aircraft. The trend of the right roll is almost the same when compared with the experimental data. CFD results shows a maximum roll angle value of 5.76 whereas experimental results show a maximum of 6.5 degrees. Although the trend is very much same but

still results show a minor discrepancy from the experimental values. The difference in data values start around 0.052 seconds just about when the ejector forces are vanished. The roll angle is especially difficult to model because the moment of inertia about the roll axis is much smaller than that of the pitch and yaw axes. Consequently, roll is very sensitive to errors in the aerodynamic force prediction.

The trend for the yawing moment which is also acting towards the left side of the wing is again the same as experimental data but there is some discrepancy with the experimental results. This difference increases with time and shows a maximum discrepancy at t=0.33 seconds.

Difference between CFD and experimental results is due to the presence of sting. In CFD no sting is modeled. So, this minor difference can be neglected. The second source of error is in the experimental data. Although the computational process is time accurate the wind-tunnel data is not. The data was taken with the Captive Trajectory Simulation (CTS) by the pitch-pause method, which is not time accurate but quasi-steady same as concluded by Lijewski *et al.* (1994).

4.2 Effect of Variation of Ejection Forces

After validation, store trajectory is simulated at different combinations of Ejection Forces. Range for both Forward and Rearward Ejection Forces is set from 0 to 42 KN and 20 cases are analyzed.

There is no significant change in the horizontal displacement of store if Forward or Rearward

Ejection Forces are changed as shown in Fig. 10.

After t=0.052 sec, effect of ejection forces is vanished off and store is only under the influence of aerodynamic forces. With greater angle of attack of store drag acting on it increases which is the main reason for increase in backward movement of the store. Moreover, backward movement of the store does not have any safety issues as far as store separation is considered.
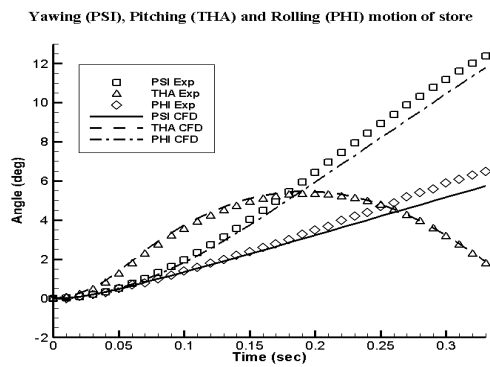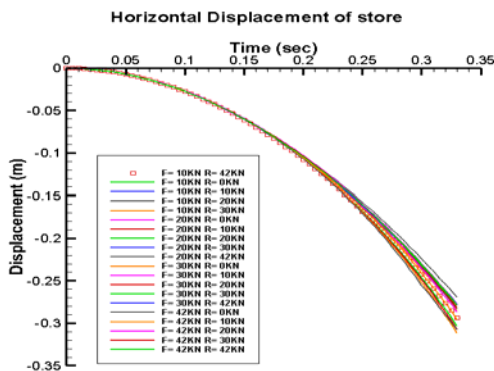

Fig. 9. Trajectory of the angular orientations.

Fig. 10. Trajectory of the center of gravity (X) at different combinations of Ejection Forces.
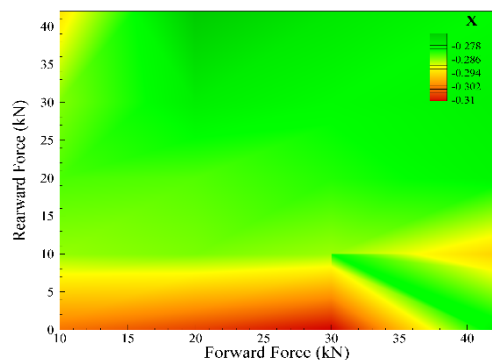
Fig. 11. Contours of Horizontal Displacement (X) at different combinations of Ejection Forces.

Figure 11 shows the maximum downstream movement of store after being separated from the wing at time t=0.33 sec. By analyzing all 20 different cases, maximum backward movement of

the store is found to be -0.31 m for case in which forward and rearward ejection forces are 30 KN and 0 KN respectively.

There is no significant change in the sideways displacement of the store by changing the Forward and Rearward Ejection Forces as shown in Fig. 12. In all 20 cases store is rolling right after separation. When Forward Ejection Force is greater than Rearward Ejection Force then store drops in nose down condition. Because of nose down and right rolling condition pressures on right side of the store are greater than left side which is the cause of increase in inboard displacement of the store.
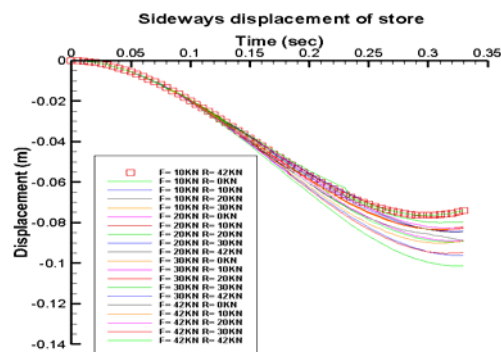

Fig. 12. Trajectory of the center of gravity (Y) at different combinations of Ejection Forces.

Figure 13 shows the maximum inward movement of store after being separated from the wing at time t=0.33 sec. By analyzing all 20 cases maximum inward sideways displacement is found out to be -0.10 m for case in which forward and rearward ejection forces are 10 KN and 0 KN respectively, which is well within safety limits.
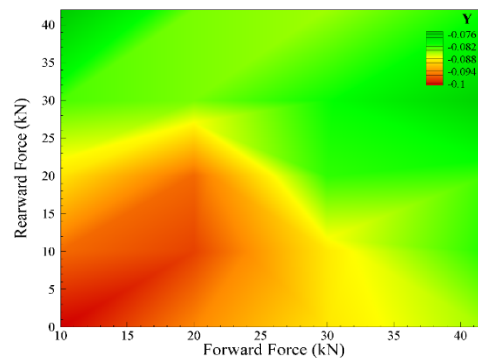

Fig. 13. Contours of Sideways Displacement (Y) at different combinations of Ejection Forces.

By analyzing all 20 cases, after 0.33 sec store is moved downward to a distance of more than 1 meter (which is quite safe) except one case in which Forward and Rearward Ejection Forces are 10 KN and 0 KN respectively as shown in Fig. 14. In the said case, maximum downward displacement after 0.33 sec is found out to be 0.8897 m which is considered to be dangerous as store is close to pylon.
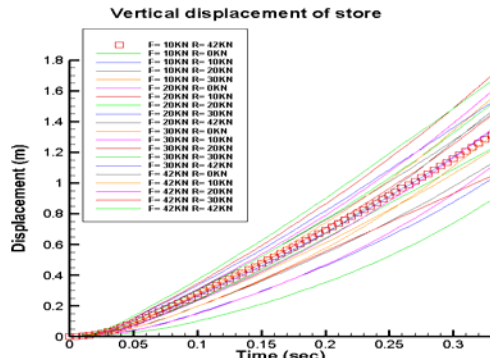
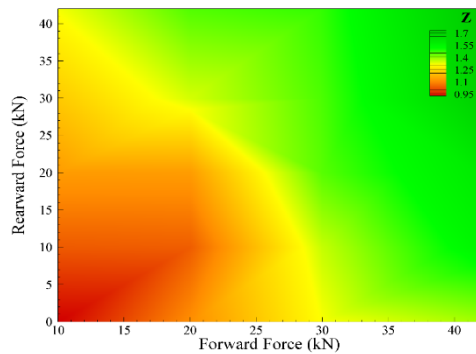**Fig. 14. Trajectory of the center of gravity (Z) at different combinations of Ejection Forces.**

Fig. 15. Contours of Vertical Displacement (Z) at different combinations of Ejection Forces.

The yaw angle is termed as PSI. In all 20 cases maximum yaw angle achieved is found out to 14.02 deg. Four cases i.e. F=10KN and R=0KN, F=10KN and R=10 KN, F=20KN and R=0KN and F=20KN and R=10KN maximum yaw angle is found out to be more than 13 degrees and are considered to be unsafe as shown in Fig. 16.
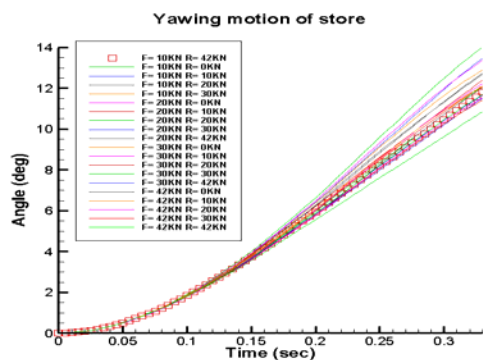
Fig. 16. Trajectory of the angular orientation (psi) at different combinations of Ejection Forces.

Before t=0.05 sec ejection forces are more dominant as compared to aerodynamic forces so greater the magnitude of Ejection Forces greater will be downward displacement of the store. But after t=0.05 sec store is only under the influence of aerodynamic forces so with greater angle of attack of store lift force acting on it increases which is the

main reason for decrease in vertical displacement of the store. By increasing the magnitude of forward ejection force only vertical displacement increases and store separates safely from the wing. Figure 15 shows the maximum downward movement of store after being separated from the wing at time t=0.33 sec.

Figure 17 clearly depicts that yawing motion of store is inversely proportional to magnitude of forward and rearward ejection force. When ejection forces are less in magnitude then aerodynamic forces are dominant and pressures on left side of the store are less as compared to right side. By decreasing forward and rearward ejection forces, yawing motion of the store is enhanced which increases its chances to touch the other stores attached to wing. For safety it is recommended that forward and rearward ejection forces should be more than 20 KN each in magnitude.
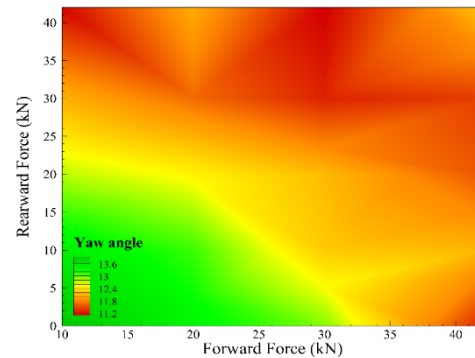

Fig. 17. Contours of Yawing motion at different combinations of Ejection Forces.

The pitch angle is termed as Theta. Pitching motion of store for all 20 cases is shown in Fig. 18. When Forward Ejection Force less than Rearward Ejection Force then store drops in nose up condition. As angle of attack of store increases then lift acting on it increases and so does the pitch angle.
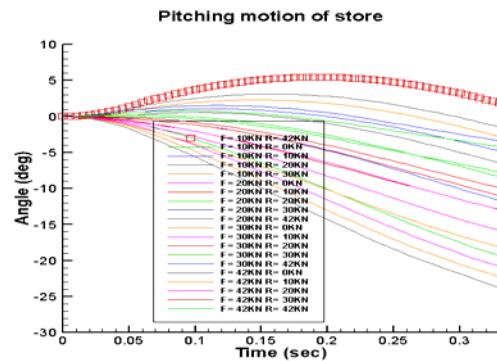

Fig. 18. Trajectory of angular orientation (Theta) at different combinations of Ejection Forces.

There is only one case i.e. F=10 KN and R=42 KN in which there is no nose down movement (Negative pitch angle). If we consider store as bomb then it is desirable that bomb should be

dropped in nose up condition so that it glides a quite distance and enables the pilot to drop the bomb safely and accurately from a far distance. So, the above-mentioned case is ideal for dropping heavy bomb.

If store is considered to be an empty fuel tank which is low in weight then it should be dropped in nose down condition because nose up condition increase the lift of empty fuel tank which increases the chances of its collision with pylon. So, all cases except above-mentioned case are favorable.

Figure 19 depicts that for nose up drop of store Rearward Ejection Force should be more in magnitude as compared to forward ejection force e.g. for case in which forward and rearward ejection forces are 10 KN and 42 KN respectively. Nose up angle of store after being separated from wing is inversely proportional to magnitude of forward ejection force. By increasing forward ejection force, nose up angle of store decreases.
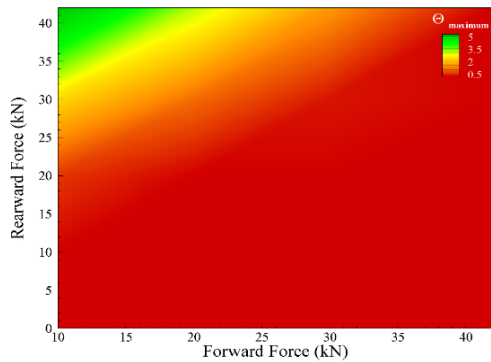

Fig. 19. Contours of pitch up ($\theta_{maximum}$) at different combinations of Ejection Forces.

Figure 20 shows that nose down angle of store after being separated from the wing depends more on rearward ejection force as compared to forward ejection force. By decreasing rearward ejection force pitch down angle increases as they are inversely proportional to each other.
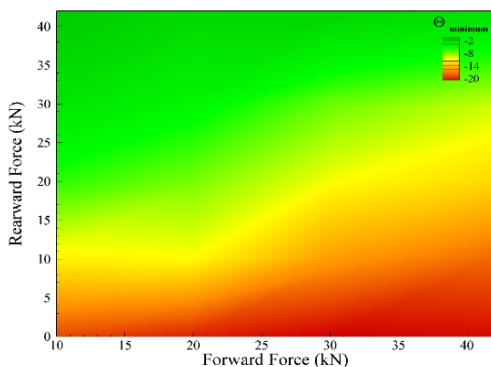

Fig. 20. Contours of pitch down ($\theta_{minimum}$) at different combinations of Ejection Forces.

The rolling motion is termed as PHI. By analyzing all cases as shown in Fig. 21 maximum roll angle is found out to be 5.75 deg. Rolling motion of the store is purely generated by aerodynamic forces. When aerodynamic forces are dominant as compared to Ejection Forces greater will be rolling motion. From stability point of view, greater the roll angle greater will be the stability.
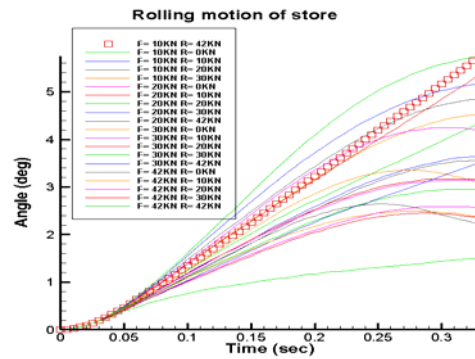

Fig. 21. Trajectory of the angular orientation (phi) at different combinations of Ejection Forces.

Figure 22 clearly depicts that rolling motion of the store after being separated from the wing depends more on forward ejection force as compared to rearward ejection force. Greater the magnitude of forward ejection force smaller will be the rolling angle.
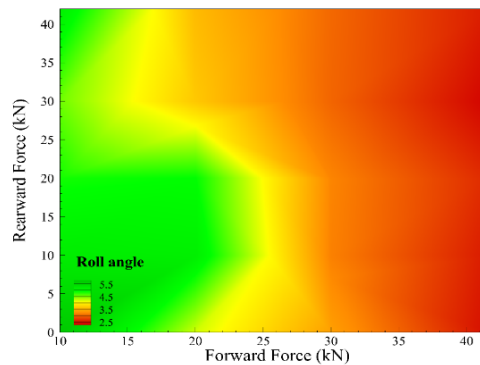

Fig. 22. Contours of rolling motion at different combinations of Ejection Forces.

4.3 Effect of Leading-Edge Flaps

Afterwards geometry is changed by introducing leading-edge Flaps (LEFs) but same ejection forces (as experimental) and store separation trajectory is simulated. Five cases are selected from the work of Axelson and Stevens (1954). Geometry of five cases is shown in Fig. 23.

Details of five LEFs cases are shown in Table 2 and their respective 3D models in Fig. 24: -

By introducing LEF in all five cases, the drag force acting on the store increases so horizontal movement of the store also increases. Hence the store backward movement is enhanced. Same trend is also observed in Fig. 25.
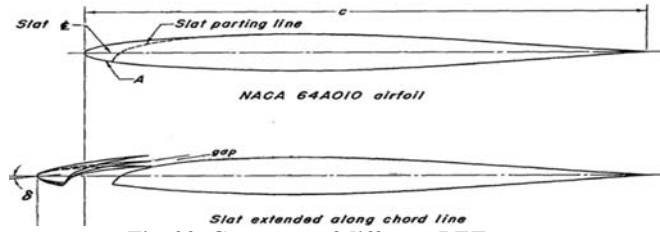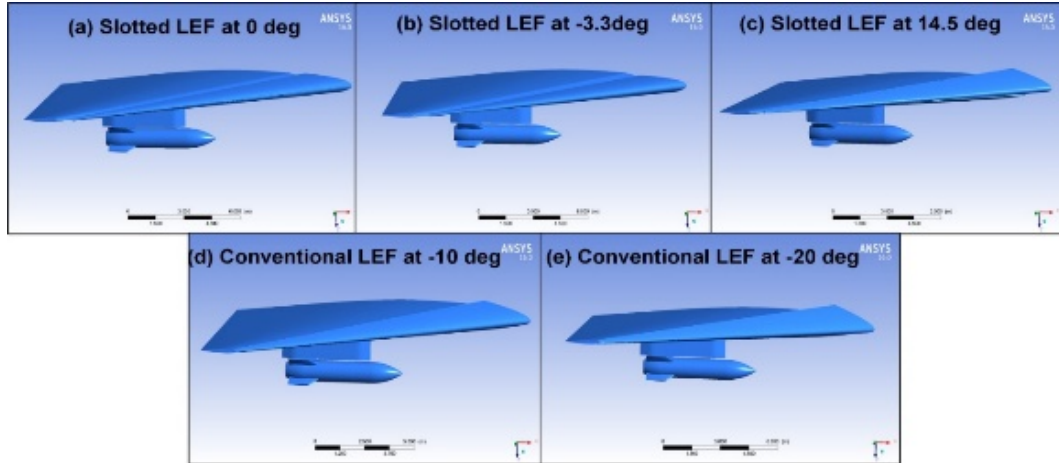
Fig. 23. Geometry of different LEF cases.

Fig. 24. 3D models of different LEF cases.

Table 2 Details of different LEFs cases

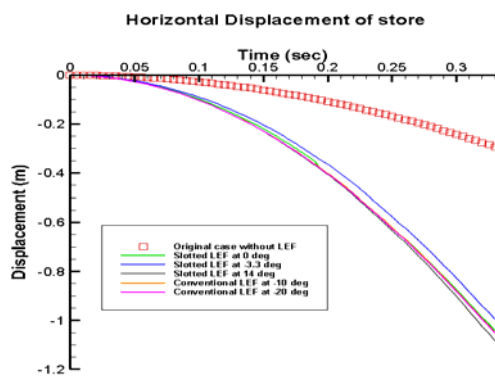| S. No	Case	gap (meters)	Angle δ (deg)
1.	Slotted LEF at 0 deg	0.019431	0^0
2.	Slotted LEF at -3.3 deg	0.019431	-3.3^0
3.	Slotted LEF at 14 deg	0.019431	14^0
4.	Conventional LEF at -10 deg	0.00	-10^0
5.	Conventional LEF at -20 deg	0.00	-20^0

Fig. 25. Trajectory of the center of gravity (X) at different cases of LEFs.
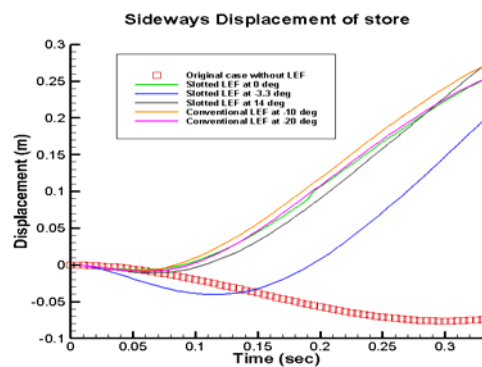

Fig. 26. Trajectory of the center of gravity (Y) at different cases of LEFs.

With the introduction of LEF in all five cases store first moves slightly towards inboard and then moves outward afterwards. Because of LEFs there is a decrease in velocities under the wing which increases pressures on left side of store as compared to right side. Thus, outboard movement of store is enhanced which increases the safety related to store separations as shown in Fig. 26.

In all five cases, store drops in nose down condition which decreases the lift force on the store. Less magnitude of lift force increases the downward movement of store and safety related to store

separation is enhanced as shown in Fig. 27.

Maximum yaw angle achieved in all five cases of LEFs is observed to be 12.14 deg which is well within safety limits as shown in Fig. 28. However, with introduction of LEF yaw angle in all five cases is quite high before 0.06 sec when store is close to wing and is under the effect of both ejector and aerodynamic forces.
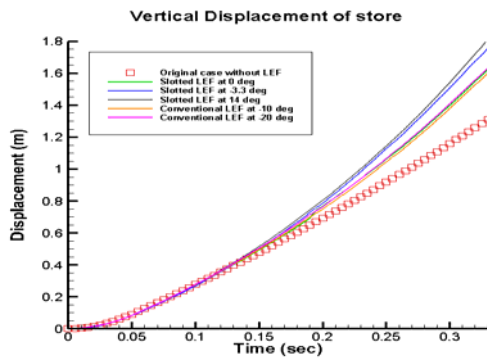

Fig. 27. Trajectory of the center of gravity (Z) at different cases of LEFs.
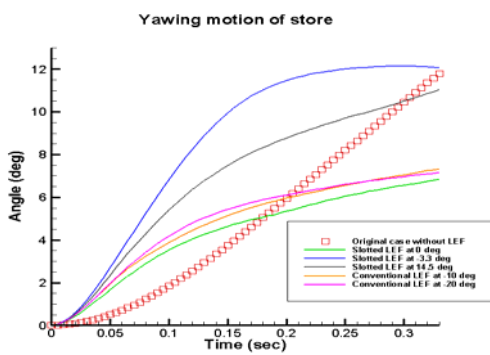

Fig. 28. Trajectory of the angular orientation (psi) at different cases of LEFs.

With introduction of LEF in all five cases store drops in nose down condition as shown in Fig. 29. LEFs increases the dominancy of aerodynamic forces as compared to Ejection Forces. As discussed earlier nose down drop position is not desirable as far as store is considered to be a bomb. However, store being an empty drop tank wings with LEFs are more useful.
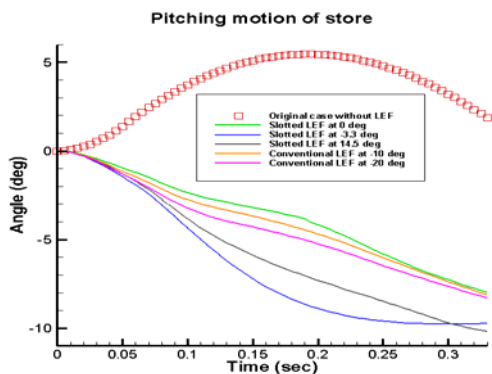

Fig. 29. Trajectory of the angular orientation (Theta) at different cases of LEFs.

By introducing the LEF in all five cases behavior of rolling motion of store is changed from linear to sinusoidal (positive and negative roll angle) as shown in Fig. 30. This sinusoidal rolling motion reduces the directional stability of the store.
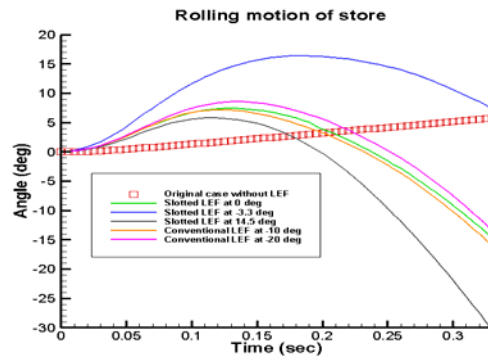

Fig. 30. Trajectory of the angular orientation (phi) at different cases of LEFs.

5.   CONCLUSION

In the current study, store separation trajectory results were analyzed and compared with the experimental data. The store moves backward, downward and towards inboard after separation and the results showed good agreement with the experimental results whereas there was small discrepancy observed in the linear and angular displacements due to no sting modeling in CFD analysis and source of error in the experimental data (pitch-pause method). Moreover, store separation trajectory was analyzed by changing the magnitude of Ejection Forces and by varying the geometry (introducing leading-edge Flaps). The results thus obtained confirmed that Ejection Forces and Leading-Edge Flaps have significant effect on trajectory of store after being separated from aircraft. Safety related to store separation can be enhanced by increasing the magnitude of forward ejection force as compared to rearward ejection force or by introducing Leading Edge Flaps as store will drop in nose down condition. Hence, we can conclude that presented solution strategy can be efficiently employed to predict store separation features.

REFERENCES

Axelson, J. A. and G. L. Stevens (1954). Investigation of a Slat in Several Different Positions on an NACA 64A010 Airfoil for a Wide Range of Subsonic Mach Numbers, *Technical Note 3129 of National Advisory Committee for Aeronautics*.

Bachelor, G. K. (2000). *An Introduction to Fluid Dynamics*, Cambridge.

Cenko, A. (2010). Store separation lessons learned during the last 30 years, *27th International Congress of the Aeronautical Sciences*, Nice, France.

Covert, E. E. (1981). Conditions for Safe Separation

of External Stores, *Journal of Aircraft, AIAA* 18(8), 81-4216.

Demir, G. and N. Alemdaroğlu (2015). CFD solutions to store separation problem, *8th Ankara International Aerospace Conference*, AIAC-2015-095.

Demir, H. O. (2004), Computational fluid dynamics analysis of store separation. *M. S. Thesis*, Middle East Technical University, Ankara, Turkey.

Fox, J. H. (2000). Generic Wing, Pylon, and Moving Finned Store, Verification and Validation Data for Computational Unsteady Aerodynamics, *RTO-TR-26*, St. Joseph Ottawa/Hill, Canada.

Hall, L. H., C. R. Mitchell and V. Parthasarathy (1997). An unsteady simulation technique for missile guidance and control applications, 35th Aerospace Sciences Meeting and Exhibit, *AIAA* Paper 97-0636, Reno, NV, U.S.A.

Heim, E. R. (1991). CFD Wing/Pylon/Finned Store Mutual Interference Wind Tunnel Experiment, *Defense Technical Information Center*, AEDC-TSR-91-P4.

Koomullil, R., G. Cheng, B. Soni, R. Noack and N. Prewitt (2008). Moving-body Simulations Using Overset Framework with Rigid Body Dynamics, *Journal of Mathematics and Computers in Simulation*, Volume 78 Issue 5-6, Pages 618-626.

Launder, B. E. and D. B. Spalding (1974). "The numerical computation of turbulent flows", *Journal of Computer Methods in Applied Mechanics and Engineering* 3(2), 269-289.

Lijewski, L. E. and N. E. Suhs (1994). "Time-Accurate Computational Fluid Dynamics Approach to Transonic Store Separation Trajectory Prediction,'' *Journal of Aircraft* 31(4), 886-891.

Mahmood, O., J. Masud and Z. Toor (2018). Trajectory simulation of a standard Store and Generic Wing Pylon using CFD, *2018 AIAA Aerospace Sciences Meeting*, AIAA 2018-1273, Kissimmee, Florida.

Parikh, P., S. Pirzadeh and N. T. Frink (1992). "Unstructured grid solutions to a Wing-Pylon-Store configuration using VGRID3D/USM3D", *AIAA,* Astrodynamics Conference Hilton Head Island, SC, USA, Paper 92- 4572.

Sejong, O. and D. Tavella (1987). Analysis of a delta wing with leading-edge flaps, *Journal of Aircraft* 24(6), 353-354.

Sunay, Y. E., E. Gülay and A. Akgül (2013). Numerical simulations of store separation trajectories using the Eglin test, *Scientific Technical Review* 63(1), 10-16.